Nanotechnology for Environmental Engineering (2020) 5:1
https://doi.org/10.1007/s41204-019-0065-3

CRITICAL REVIEWS

Silver nanoparticles adsorption by the synthetic and natural adsorbent materials: an exclusive review

Achmad Syafiuddin[1,2] · Mohamad Ali Fulazzaky[3,4] · Salmiati Salmiati[1,2] · Ahmad Beng Hong Kueh[5] · Mohammad Fulazzaky[6] · Mohd Razman Salim[2]

Received: 28 October 2019 / Accepted: 30 December 2019

Abstract

Silver nanoparticles (AgNPs) have been used in a wide range of industrial products. The release of AgNPs as antimicrobial agent into the river or lake can raise the ecological concern because they have been proven to be associated with toxicity of the aquatic animals. An exclusive review of AgNPs adsorbed by the various synthetic and natural adsorbent materials is important to understand the behaviour of AgNPs in the complex environmental conditions. The transformation of AgNPs into various forms in an aquatic environment depends on the physical, chemical, and biological characteristics of water. Many types of natural materials can be used to fabricate the adsorbents because pore structure, surface area, and active sites of functional groups of the adsorbent can be developed during the carbonisation and activation stages. The mass transfer factor and modified mass transfer factor models would be considered tools that can be used to describe the mechanism and kinetics of AgNPs adsorption onto the natural adsorbents influenced by the electrostatic and van der Waals forces. This exclusive review provides the valuable insights into future challenges of AgNPs adsorption to contribute to sustainable improvement in the management of aquatic ecosystems.

Keywords Adsorption isotherm · Adsorption kinetic · Interaction mechanism · Natural adsorbent material · Silver nanoparticles · Synthetic adsorbent material

Introduction

Nanoscale materials have in the recent decades been widely used to satisfy continual demand from a vast variety of the industrial applications [7, 13, 44, 63]. It should be due to the accelerated advancement in nanotechnology by synthesis and manipulation of the particle structure being characterised with a size range of 1–100 nm is the fundamental ways of enhancing the interaction of atoms/molecules [2]. A beneficial development of materials can promote the use of the nanoparticles for many applications such as in biomedical, catalysis, chemical industry, cosmetic, drug–gene delivery, electronic, energy science, environment, food, health care, light emitter, mechanic, nonlinear optical device, optic, photoelectrochemical, single-electron transistor, and space industry [2, 3, 65]. Application of silver nanoparticles (AgNPs) has currently been an enormous attraction and intensively explored to be used for the various industrial products because they have favourable physical, chemical, and biological properties [33, 44, 46, 63, 88]. Some applications of AgNPs are: (1) in textiles such as anti-stain, medical textiles, and UV blocking (2) in biomedical

✉ Mohamad Ali Fulazzaky
mohamad.ali.fulazzaky@tdtu.edu.vn

1 Department of Water and Environmental Engineering, Faculty of Civil Engineering, Universiti Teknologi Malaysia (UTM), 81310 Johor Bahru, Johor, Malaysia

2 Centre for Environmental Sustainability and Water Security (IPASA), Research Institute for Sustainable Environment, Faculty of Civil Engineering, Universiti Teknologi Malaysia (UTM), 81310 Johor Bahru, Johor, Malaysia

3 Department for Management of Science and Technology Development, Ton Duc Thang University, No. 19 Nguyen Huu Tho Street, Tan Phong Ward, District 7, Ho Chi Minh City, Vietnam

4 Faculty of Environment and Labour Safety, Ton Duc Thang University, No. 19 Nguyen Huu Tho Street, Tan Phong Ward, District 7, Ho Chi Minh City, Vietnam

5 Department of Civil Engineering, Faculty of Engineering, Universiti Malaysia Serawak, 94300 Kota Samarahan, Serawak, Malaysia

6 Department of Chemical Engineering, Faculty of Industrial Technology, Bandung Institute of Technology, Jalan Ganesha No. 10, Bandung 40132, Indonesia

Published online: 04 January 2020

application such as antibacterial, antifungal, cancer therapy, cell imaging, diagnosis, and drug delivery, (3) in health care such as UV protection, topical ointments and cream, and nutraceutical, (4) in agricultural food production such as food packaging, food quality analysis sensors, and interactive food, (5) in catalysis such as fuel additive, fuel cell, and hydrogen production, and (6) in environment remediation such as water disinfection and wastewater treatment [9, 38].

A huge amount of AgNPs discharged into the environment could be due to the surge in usage of them [61, 80]. The presence of AgNPs has been found in the environment such as in the river, wastewater, washing water, seawater, and reservoir [5, 11, 80, 87]. A washing water contained AgNPs in washing machine released into the wastewater collecting system can harm healthy beneficial bacteria involved in the treatment process, endangered aquatic organisms in the lakes, streams, and other freshwater ecosystems [81, 95]. Because the release of AgNPs from washing entering the wastewater treatment plants around the world has been predicted to be around 270 tonnes/year [5], the project sustainability of AgNPs removal from waters would be the major challenge in many developed and developing countries.

Many processes like adsorption, aeration, and coagulation have been proposed for the removal of AgNPs from waters [12, 50, 60, 62, 87]. However, the aeration process is more complicated method when comparing with the process of both coagulation and adsorption because the removal of AgNPs processed in a sequencing batch reactor could be rather time-consuming. The coagulation process of using coagulant such as either aluminium sulphate, ferric chloride, polyaluminium chloride, or polyferric sulphate can ally with a new source of pollution in the environment. Therefore, the adsorption process is the best candidate for safe removal of AgNPs from water and uses the non-toxic materials to produce a nearly zero-waste. The application of the various kinetic and isotherm models has been reviewed for better understanding on the kinetics and mechanism of AgNPs adsorption by the synthetic and natural materials from waters [89]. The objectives of this paper are: (1) to conduct an exclusive review of AgNPs adsorption regarding (i) the interaction of AgNPs with halides, oxygen, and sulphide; (ii) the different types of adsorbents; (iii) the validity of the kinetic and isotherm models; (iv) the distinct mechanisms of the interactions; and (v) the factors affecting the adsorption of AgNPs and (2) to provide the valuable insights into the future challenges of AgNPs adsorption.

Interaction of AgNPs with halides, oxygen and sulphide

AgNPs in water can transform in the form of either Ag^+ or Ag^0 depending on the physical, chemical, and biological conditions, as illustrated in Fig. 1 [37, 56]. This chapter reviews the interaction of AgNPs with halides, oxygen, and sulphide to get better understanding of the effect of different water conditions on the adsorption of AgNPs [10].

Interaction of AgNPs with halides

AgNPs can react with either Cl^- or Br^- to form a stable complex salt capable of precipitating as $AgCl^-$NPs or $AgBr^-$NPs [71]. The chemical reaction of Ag^+ with Cl^- can transform it into either $AgCl^{2-}$, $AgCl_3^{2-}$, $AgCl_4^{3-}$, or AgCl precipitate depending on the amount of Cl^- in water, whereas seawater contains approximately 500 mM NaCl and surface water contains in the range of 1–10 mM NaCl. The dissolution kinetics of AgNPs decrease with decrease in Cl^- concentration and lead to scavenging of Ag^+ and the formation of an AgCl passivation layer. A high amount of Cl^- in water can increase the dissolution kinetics of AgNP to result stable complex salt capable of capturing certain amount of Cl^-. AgNPs can react with Br^- to form either $AgBr^-$NPs or AgBr depending on the nature of water environment where the attractive force between AgNPs and Br^- is controlled by the amount of AgBr precipitate on the surface of AgNPs [71]. AgNPs are not chemically stable in the water environment and react strongly with Cl^- and Br^- once the Ag^+ is oxidised [48]. The chemical reactions can be described as:

$$AgNPs + H_2O_2 + Cl^- \rightarrow AgCl^-NPs + H_2O \quad (1)$$

$$AgNPs + H_2O_2 + Br^- \rightarrow AgBr^-NPs + H_2O \quad (2)$$

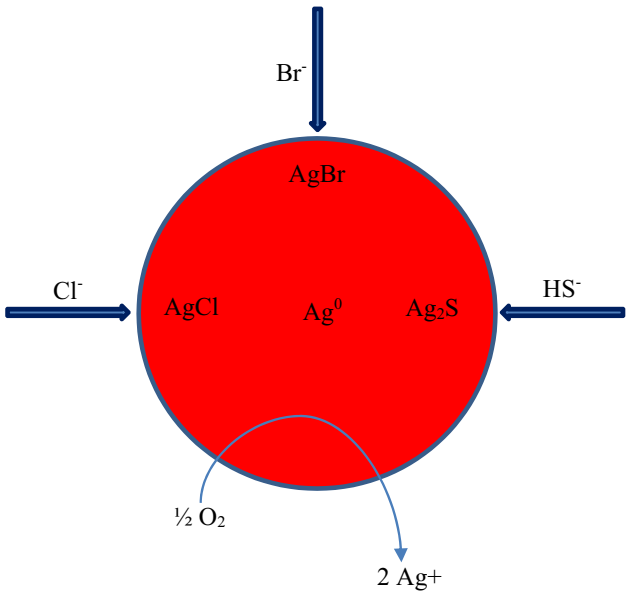

Fig. 1 Schematic of AgNPs transformation in water

Equations (1, 2) exhibit the potential application of AgNPs to remove Br^- and Cl^- from waters. The performance of Br^- removal higher than that of Cl^- could be due to the solubility of AgBr which is lower than that of AgCl. It has been reported that the toxicity of AgNPs to *E. coli* decreases with increase in Cl^- ions in water due to the Cl/Ag ratio that controls dissolution rate more than aggregation state and can suggest an ion effect rather than a nanoparticle effect on the toxicity of silver species, while Cl^- can react with AgNPs to form a stable complex salt in the form of $AgCl^-$NPs [48, 71].

Interaction with oxygen

AgNPs can react with O_2 to form Ag_2O layer on the surface of AgNPs because the oxidative dissolution of AgNPs caused by the presence of O_2 in carbonated water under oxic condition exists [35]. Ag_2O layer can dissolve in water when Ag^+ concentration is low. The change in Gibbs free energy of the Ag-contained solution during the transformation of Ag^0 to Ag_2O with $\Delta G^0_{298^\circ K}$ of -11.25 kJ mol^{-1} occurs with the presence of O_2 and is thermodynamically unstable. Ag^+ is stable in aqueous solution and solid state, while Ag^{2+} is less stable and can react with water to form Ag^+. The oxidative dissolution rate of AgNPs at low pH increases with increase in dissolved O_2 in water due to that the rate of AgNPs dissolution under oxic conditions can be stimulated with the significant amounts of two chemical species H^+ and O_2 involved in the reaction. The transformation of Ag^+ to Ag_2O can be described [80] as:

$$2Ag^+ + 2OH^- \rightarrow Ag_2O + H_2O \quad (3)$$

The kinetics of oxidative dissolution of AgNPs may be controlled by the presence of chlorine, surfactant, natural organics, hydrogen peroxide, and the size of AgNPs [26]. The decrease in AgNPs size can enhance the oxidative dissolution because the surface-to-volume ratio increases [15]. The presence of surfactant and natural organics may shield the surface of AgNPs from O_2 and the dissolution of Ag_2O layer; hence, the oxidative dissolution of AgNPs decreases [35].

Interaction with sulphide

AgNPs can react with sulphide through sulphidation to form Ag_2SNPs, while water can enhance the process of sulphidation [47, 48]. A high solubility of H_2S in the water can increase the probability of Ag^0–H_2S contact due to that H_2S can easily diffuse through the surface of AgNPs. Kinetics of sulphidation are affected by the surface orientation and the steps of facilitating nucleation [47]. Despite it needs to have a more fundamental understanding of the sulphidation of AgNPs, the presence of sulphide can affect the properties of AgNPs. In situ transmission electron microscopy observations of fracture in AgNPs shown that Ag_2S forms the nanobridges between AgNPs leading to chain-like fractal structures of consecutively composing the AgNPs surfaces oxidise, AgNPs dissolve partially and reprecipitate of Ag_2S nanobridge between AgNPs [49]. The sulphidation reaction of AgNPs can be described [53] as follows:

$$2Ag + \frac{1}{2}O_2 + HS^- \rightarrow Ag_2S + OH^- \quad (4)$$

Types of adsorbents

In general, the adsorption of AgNPs from waters can be performed using the methods of batch experiment and hydrodynamic column. Both methods can be used to study the transport behaviours of AgNPs during the adsorption process [93]. Using the batch adsorption experiments permits us to easily investigate the adsorption of AgNPs. Figure 2 shows the schematic of AgNPs adsorption by batch experiment. Various types of the adsorbents have been employed for the adsorption of AgNPs. The adsorption of AgNPs by Norit-CA1 in a closed vial of 4 mL at 20 °C for 12 h can attain 100% efficiency because the presence of mesoporous structure in Norit-CA1 contributes to an effective surface area [27]. The batch experiment of AgNPs adsorption by glass beads of being characterised by the size range of 70–110 µm for 6 h can reach 75% efficiency, and this may relate to the presence of hydrogen bond between oxygen in the carbonyl groups of polyvinylpyrrolidone and silanol groups of glass beads [72]. The use of poly(vinyl alcohol)/gum karaya electrospun plasma-treated membrane to remove AgNPs from

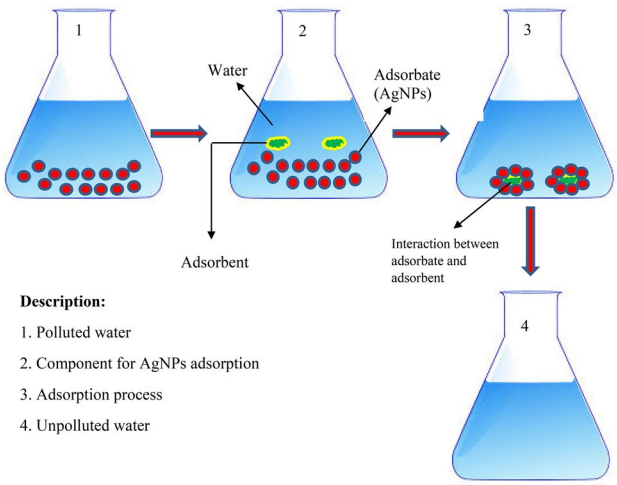

Fig. 2 Schematic of AgNPs adsorption by batch experiment

water can reach 78.1% efficiency [68]. The batch experiment of AgNPs adsorption by sodium montmorillonite nanoclay in 25 mL water for 10 min can remove up to 71.4 mg g^{-1} of AgNPs as the maximum adsorption capacity at neutral pH of 7 [97]. The adsorption of AgNPs by copper-based metal organic frameworks in batch reactor with a pH range of 1–7 can attain the maximum capacity of 83 mg g^{-1} [12]. The removal of AgNPs from water by adsorbing onto the aged magnetic Fe_2O_3 particles can attain an adsorption capacity in the range of 19.9–62.8 mg g^{-1} after reaching 20 min of equilibrium time and has a removal efficiency in the range of 63.3–99.9%, while the removal and recovery of AgNPs from water are still consistent with four cycles of adsorption–desorption [100]. Table 1 summarises the different types of adsorbent materials for the adsorption of AgNPs. Despite that the use of the synthetic and natural materials could be useful for the adsorption of AgNPs from water, it has been shown that the synthetic materials are favoured due to their structure and advanced properties can be fabricated during the carbonisation and activation stages. It can be concluded according to the experiments of using five natural materials and seventeen synthetic materials (see Table 1) that the adsorption efficiency of the synthetic materials to remove the AgNPs species from water is generally better than that of the natural materials. Therefore, efforts to increase the adsorption capacity of the natural adsorbent-based materials by modifying the characteristics of heterogeneous surface and structure of the porous materials are a challenge in the future.

Validity of the adsorption kinetics and isotherm models

Adsorption kinetics

This work reviewed the adsorption kinetics within the framework of four adsorption kinetic equations, such that: (1) pseudo-first-order model, (2) pseudo-second-order model, (3) Elovich model, and (4) intraparticle diffusion model.

The expression of pseudo-first-order model can be written [85] as:

$$q_t = q_e\left[1 - \exp\left(-k_{p1}t\right)\right] \tag{5}$$

where q_t is the adsorption capacity of the adsorbent (in mg g^{-1}) at time t of running the experiment (in min), q_e is the adsorption capacity of the adsorbent at equilibrium (in mg g^{-1}), and k_{p1} is the rate constant of pseudo-first-order model (in min^{-1}).

Table 1 Types of the adsorbents for AgNPs adsorption

Adsorbent	References
Natural material	
Aeromonas punctata	Khan et al. [41]
Activated carbon (Norit-CA1)	Gicheva and Yordanov [27]
Natural clinoptilolite	Ruíz-Baltazar et al. [77]
Aspergillus niger	Gomaa [28]
Activated sludge	Oh et al. [66]
Synthetic material	
Aged iron oxide magnetic particles	Zhou et al. [100]
Glass beads	Polowczyk et al. [72]
Plasma modified nanofibers	Padil et al. [69]
Sodium montmorillonite nanoclay	Zarei and Barghak [97]
Nitrogen-rich core–shell magnetic mesoporous silica	Zhang et al. [98]
Mussel-inspired Fe_3O_4–polydopamine core–shell microspheres	Wu et al. [94]
Metal organic framework (HKUST-1)	Conde-González et al. [12]
Poly(vinyl alcohol) membranes	Mahanta and Valiyaveettil [57]
Poly(vinyl alcohol)/gluten nanofibers	Dhandayuthapani et al. [14]
Biomimetic metal oxides	Mallampati and Valiyaveettil [58]
Amine-functionalized block copolymers	Qureshi et al. [73]
Multiwalled carbon nanotubes	Hassan and Farghali [32]
Polycaprolactone electrospun fibre mats	Liu et al. [51]
Functionalized magnetite particles	Lopes et al. [55]
Polyethyleneimine (PEI)-functionalized paper	Setyono and Valiyaveettil [78]
Nanoporous silica	Sim et al. [84]
Bimodal nanoporous silica	Sim et al. [84]

Modelling the adsorption kinetics of pseudo-second order can be expressed [85] as:

$$q_t = \frac{k_{p2} q_e^2 t}{1 + k_{p2} q_e t} \tag{6}$$

where k_{p2} is the rate constant of pseudo-second order (in min^{-1}).

The Elovich equation can be written [96] as:

$$q_t = \frac{1}{\beta} \ln(\alpha\beta) + \frac{1}{\beta} \ln(t) \tag{7}$$

where α is the initial adsorption rate of solute onto adsorbent (in mg g^{-1} min^{-1}) and β is the desorption constant of the Elovich equation (in g mg^{-1}).

The equation of intraparticle diffusion may take the formula [96] of:

$$q_t = k_{ip} \sqrt{t} + c_{ip} \tag{8}$$

where k_{ip} is the coefficient of measuring the intraparticle diffusion (in mg g^{-1} min^{-1}) and c_{ip} is the constant of intraparticle diffusion (in mg g^{-1}).

The batch experiments of AgNPs adsorbed on the natural clinoptilolite with different initial AgNPs concentrations of 1, 2, 3, 4 mg L^{-1} were conducted to validate the four adsorption kinetic models. The accuracy of each model can be verified with the R^2 value ranged from 0.76 to 0.90 for the pseudo-first-order model, ranged from 0.97 to 0.99 for the pseudo-second-order model, ranged from 0.88 to 0.94 for the Elovich model, and ranged from 0.91 to 0.95 for the intraparticle diffusion model. The experimental data fitted better with the pseudo-second-order model to get verified from its R^2 value ranged from 0.97 to 0.99 could this model be a better kinetic expression when compared to other kinetic expressions and may suggest the formation of chemical bonds between adsorbent and adsorbate to form a monolayer on the natural clinoptilolite surface [77].

The AgNPs adsorption onto the commercial glass beads in batch experiment using the initial concentrations of 500 and 1000 mg L^{-1} has been predicted by using two models of pseudo-first-order and pseudo-second-order. The adsorption kinetic data fitted well with pseudo-second-order model due to its R^2 value of around 0.99 were verified, while the experimental data can fit with pseudo-first-order model with R^2 value in the range of 0.77–0.87 [72]. The adsorption kinetics of AgNPs in batch experiments by the core–shell microspheres of mussel-inspired Fe_3O_4–polydopamine have been also described using two models of pseudo-first-order and pseudo-second-order. The adsorption capacity of 112.95 mg g^{-1} predicted using the pseudo-first-order model is higher than that of 96.15 mg g^{-1} predicted using the pseudo-second-order model, while the regression analysis using the pseudo-second-order model with R^2 value of 0.99 provides the best fit to experimental data when compared to that using the pseudo-first-order model with R^2 value of 0.66 [94]. The capacity of AgNPs adsorption by the silica of nitrogen-rich core–shell magnetic mesoporous in batch reactor predicted using the pseudo-first-order model of having q_e value of 317.3 mg g^{-1} with R^2 value of 0.99 confirms a better fit to the experimental data comparing with that using the pseudo-second-order model of having q_e value of 371.7 mg g^{-1} with R^2 value of 0.84 [98].

The kinetics of AgNPs adsorbed on the nanofibre membranes composing polyvinyl alcohol (PVA) and natural gum karaya were described using both the models of pseudo-first-order and pseudo-second-order to show that the adsorption capacity of 39.84 mg g^{-1} predicted using the pseudo-second-order model is very close to the experimental data verification of 38.62 mg g^{-1} and the pseudo-first-order model does not allow to predict the capacity of AgNPs adsorption because the R^2 value does not quantify goodness of fit [68]. Using the pseudo-second-order model permits us to predict the maximum capacity of nanofiber membranes composing both PVA and natural gum karaya to adsorb AgNPs to increase from 143.4 mg g^{-1} before to 168.5 mg g^{-1} after treatment using the methane plasma. The best fit of experimental data to the pseudo-second-order model as verified with R^2 value of 0.99 could be the best kinetic expression because the pseudo-first-order model does not quantify a goodness of fit to the experimental data [69].

The kinetic adsorption behaviour of AgNPs deposited on amine-functionalized block copolymers was investigated to show that the capacity of AgNPs adsorption predicted using the pseudo-second-order equation is in the range of 99–117 mg g^{-1} and that predicted using the pseudo-first-order equation is the range of 44–56 mg g^{-1}. Using the pseudo-second-order equation can quantify a best fit to the data characterised with R^2 value of 0.99 [73]. The adsorption capacity of AgNPs onto poly(vinyl alcohol)–gluten hybrid nanofibers investigated using the pseudo-second-order equation ranges from 9 to 40 mg g^{-1}, depending on the amount of gluten in nanofibers. In this case, the process of establishing a curve by the pseudo-second-order equation has a best fit to a series of data points as shown in the R^2 value ranged from 0.97 to 0.99; however, the equation of pseudo-first-order cannot be used to predict the adsorption capacity of AgNPs [14]. The investigation of AgNPs deposited on *Aeromonas punctata* conducted by the batch technique at three different pHs showed the adsorption capacity at equilibrium as high as 0.47, 0.40, and 0.053 pg $cell^{-1}$ referring the mean nuclear DNA content per cell for the experiment conditioned at the pHs of 5, 7, and 9, respectively. Using the pseudo-first-order equation can predict the capacity of AgNPs adsorption better fit to the experimental data compared using the pseudo-second-order equation [41]. Figure 3

shows some examples of the kinetic adsorption behaviours of AgNPs deposited on: (a) nitrogen-rich core–shell magnetic mesoporous silica described by the pseudo-first-order kinetic model [98], (b) *Aeromonas punctata* described by the equation of pseudo-first order [41], (c) poly(vinyl alcohol)–gluten hybrid nanofibers described by the pseudo-first-order kinetic model [14], and (d) poly(vinyl alcohol)–gluten hybrid nanofibers described by the pseudo-second-order kinetic model [14]. Table 2 summarises a short overview of the kinetic adsorption behaviours of AgNPs deposited on the various adsorbents regarding the time of running the experiment and the adsorption capacity of the adsorbent at equilibrium.

Adsorption isotherms

The Langmuir, Freundlich, and Dubinin–Radushkevich isotherm equations were reviewed to describe the behaviours of AgNPs adsorption. Using the Langmuir equation permits us to describe the monolayer sorption of AgNPs occured on the homogenous surface of an adsorbent with a finite number of identical sites with the pores and can be mathematically expressed [31] as:

$$q_e = \frac{K_L q_m C_e}{1 + K_L C_e} \tag{9}$$

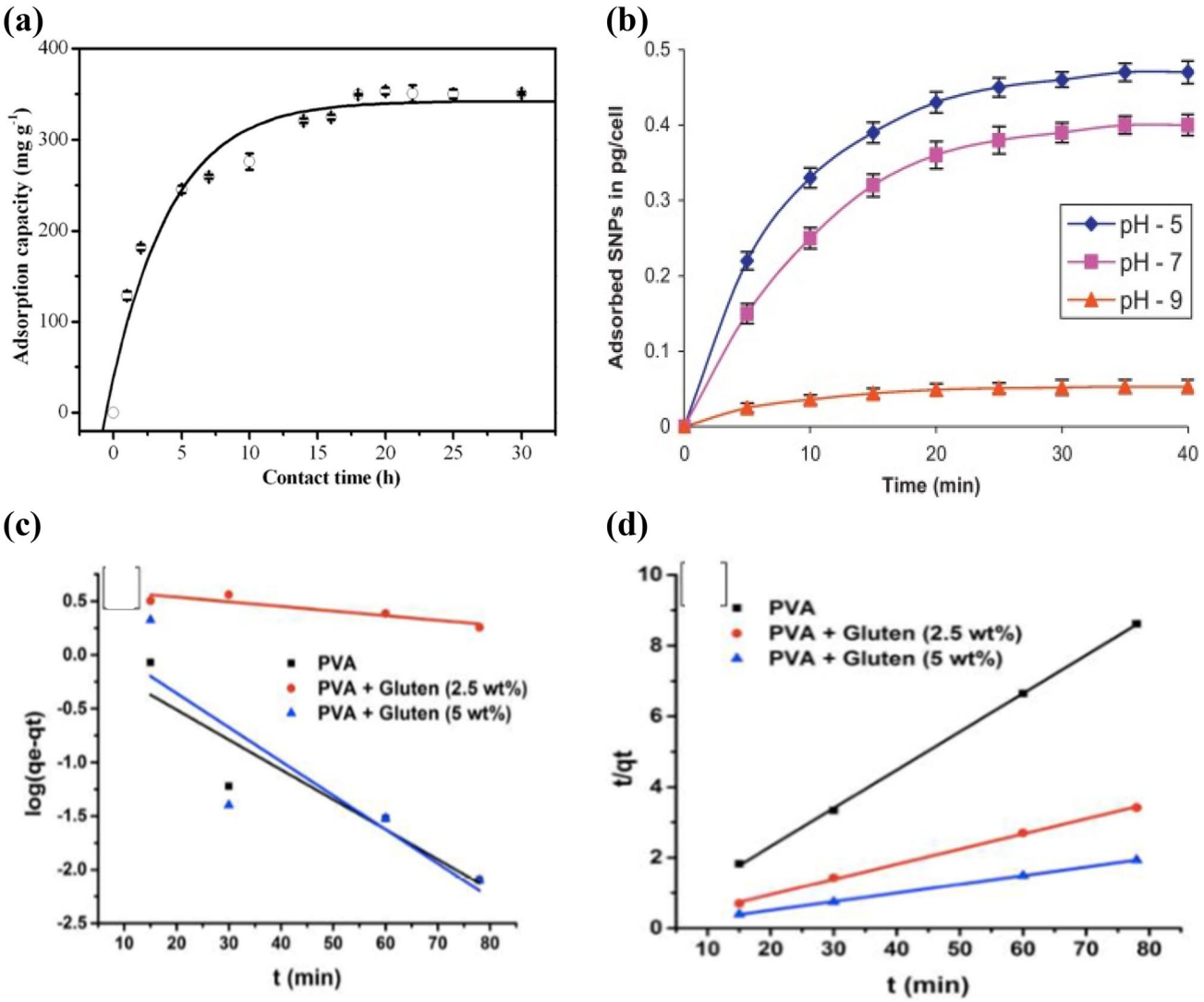

Fig. 3 Kinetic adsorption behaviours of AgNPs deposited on: **a** nitrogen-rich core–shell magnetic mesoporous silica described by the pseudo-first-order kinetic model [98], **b** *Aeromonas punctata* described by the pseudo-first-order kinetic model [41], **c** poly(vinyl alcohol)–gluten hybrid nanofibers described by the pseudo-first-order kinetic model [14], and **d** poly(vinyl alcohol)–gluten hybrid nanofibers described by the pseudo-second-order kinetic model [14]

Table 2 Kinetic adsorption behaviour of AgNPs deposited on various adsorbents

Adsorbent	t	q_e	References
Aeromonas punctata	0 to 40	0.05 to 0.47[(1)]	Khan et al. [41]
Natural clinoptilolite	0 to 180	8.38×10^{-4} to 3.61×10^{-3}	Ruíz-Baltazar et al. [77]
Activated sludge	0 to 1400	4.24 to 16.05	Oh et al. [66]
Aged iron oxide magnetic particles	0 to 90	21.50 to 67.90	Zhou et al. [100]
Glass beads	0 to 360	5.08 to 6.40	Polowczyk et al. [72]
Nanofibre membrane	0 to 180	143.40	Padil et al. [69]
Methane plasma-treated membrane	0 to 180	168.50	Padil et al. [69]
Nitrogen-rich core–shell magnetic mesoporous silica	0 to 1800	353.35	Zhang et al. [98]
Mussel-inspired Fe_3O_4@ polydopamine core–shell microspheres	0 to 2160	83.53	Wu et al. [94]
Poly(vinyl alcohol) membranes	0 to 200	56.60	Mahanta and Valiyaveettil [57]
Poly(vinyl alcohol)	0 to 180	9.50	Dhandayuthapani et al. [14]
Poly(vinyl alcohol)/gluten nanofibers (2.5 wt%)	0 to 180	24.61	Dhandayuthapani et al. [14]
Poly(vinyl alcohol)/gluten nanofibers (5.0 wt%)	0 to 180	40.25	Dhandayuthapani et al. [14]
NiO	0 to 720	54.84	Mallampati and Valiyaveettil [58]
CeO_2	0 to 720	51.04	Mallampati and Valiyaveettil [58]
ZnO	0 to 720	47.56	Mallampati and Valiyaveettil [58]
Co_3O_4	0 to 720	41.89	Mallampati and Valiyaveettil [58]
CuO	0 to 720	5.02	Mallampati and Valiyaveettil [58]
PAEA-*b*-PS	0 to 360	97.48	Qureshi et al. [73]
PAPA-*b*-PS	0 to 360	115.17	Qureshi et al. [73]
PAXA-*b*-PS	0 to 360	112.66	Qureshi et al. [73]

Remarks that the units of t are all expressed in min and the units of q_e are all expressed in mg g^{-1} except [(1)]the unit of q_e for the adsorbent of *Aeromonas punctata* is expressed in the mean nuclear DNA content (pg) per cell (pg $cell^{-1}$)

where q_e is the adsorption capacity of the adsorbent at equilibrium (in mg g^{-1}), q_m is the maximum adsorption capacity of the adsorbent per unit weight of the adsorbent (in mg g^{-1}), C_e is the concentration of adsorbate in solution at equilibrium (in mg L^{-1}), and K_L is the Langmuir constant related to the binding sites affinity (in L mg^{-1}).

Using the Freundlich equation permits us to investigate the adsorption of AgNPs on either the heterogeneous surface of a material or the surface supporting sites with varied affinities. This model assumed that stronger binding sites firstly occupy the surface of material, and then, binding strength continuously decreases with increasing the occupation of sites [83]. The Freundlich equation can be expressed in the form [31] of:

$$q_e = K_f C_e^{1/n} \tag{10}$$

where K_f is the Freundlich constant related to the sorption capacity of the adsorbent (in L g^{-1}) and n is the sorption intensity of the adsorbent (dimensionless). The value of $1/n$ is proportional to the change in effectiveness of sorption over the course of the reaction due to different equilibrium concentrations when the value of $1/n > 1$ indicated the change in adsorbed concentration is greater than that of solute concentration [64].

Using the Dubinin–Radushkevich equation permits us to distinguish the physical adsorption from chemical adsorption of the adsorbent in terms of the average free energy and can be expressed [6] as:

$$\ln q_e = \ln q_m - k\varepsilon^2 \tag{11}$$

with

$$\varepsilon = RT\ln\left(1 + \left({}^{1}/_{C_e}\right)\right) \tag{12}$$

where k is the Dubinin–Radushkevich constant related to the average free energy of adsorption (in mol kJ^{-1}), ε is the Polanyi potential (in kJ mol^{-1}), R (=8.314 J mol^{-1} K^{-1}) is the gas constant, and T is the temperature (in K).

The average free energy of adsorption can be calculated using the formula [6]:

$$E = \frac{1}{\sqrt{2k}} \tag{13}$$

where k is the average free energy of adsorption (in kJ mol^{-1}).

The isotherm AgNPs adsorption on the aged iron oxide magnetic particles in batch experiment showed that the Langmuir, Freundlich, and Dubinin–Radushkevich equations

can be evaluated based on the R^2 values of 0.98, 0.84, and 0.97, respectively. According the R^2 value, the validity of Langmuir model is better than that of Dubinin–Radushkevich model, and then, it is better than that of Freundlich model [100]. The regression analysis for the isotherm adsorption of AgNPs by the mussel-inspired Fe_3O_4–polydopamine core–shell microspheres in batch experiment can result in the R^2 values of 0.99, 0.82, and 0.97 for validating the equations of Langmuir, Freundlich, and Dubinin–Radushkevich, respectively. According to the R^2 value, the applicability of Langmuir equation is better than that of Dubinin–Radushkevich equation, and then, it is better than that of Freundlich equation. In addition, the predicted values of q_m as high as 169.5 and 180.3 mg g^{-1} were verified for the isotherm equations of Langmuir and Dubinin–Radushkevich, respectively [94]. Study on the binding properties of AgNPs to Fe_3O_4–SiO_2–PEI showed that the isotherm Langmuir and Freundlich equations can have a good fit to the experimental data points with the R^2 values of 0.98 and 0.99, respectively, from which the calculated q_m value of 909.1 mg g^{-1} can be predicted using the Freundlich equation [98]. Using the isotherm equations of both Langmuir and Freundlich permits us to describe the binding properties of AgNPs adsorbed on the sodium montmorillonite nanoclay, according to the R^2 values of 0.99 and 0.98 obtained from a regression analysis to test the applicabilities of Langmuir and Freundlich equation, respectively, whereas the q_m value of 71.4 mg g^{-1} has been predicted using the Langmuir equation [97].

The adsorption of AgNPs on *Aeromonas punctata* in batch experiment at pHs of 5, 7, and 9 was investigated using the Langmuir model which best fits the data with the R^2 value of 0.99. The predicted q_m values of 0.44, 0.38, and 0.05 pg $cell^{-1}$ were verified for the pHs of 5, 7, and 9, respectively [41]. The prediction of q_m value for the AgNPs adsorption on the Norit-CA1 using the Freundlich equation is in the range of 46 ± 16 to 65 ± 15 μg mg^{-1} and is better than that using the Langmuir equation [27]. This means that the applicability of Freundlich equation is better than that of Langmuir equation in investigating the isotherm AgNPs adsorption on the copper-based metal organic framework nanoparticles [12]. Figure 4 shows some examples of the isotherm behaviours for the adsorption of AgNPs onto: (a) aged iron oxide magnetic particles described by the Langmuir and Freundlich models [100], (b) Fe_3O_4–SiO_2–PEI described by the Freundlich model [98], (c) Norit-CA1 described by the Freundlich model [27], and (d) Norit-CA1 described by the Langmuir model [27]. Table 3 summarises a short overview of the isotherm adsorption property of AgNPs deposited on the various adsorbents regarding the concentration of adsorbate in solution at equilibrium and the maximum adsorption capacity of the adsorbent per unit weight of the adsorbent.

Distinct mechanisms of the interactions

Electrostatic interaction

An overview of the AgNPs adsorption by the synthetic and natural materials can be discussed in the context of the adsorption mechanisms, affected parameters, and adsorption behaviours for suggesting the future challenges of environmental remediation, as schematically shown in Fig. 5. An electrostatic interaction of AgNPs to adsorbent may occur when the interaction is governed by ion exchange followed by the adsorption process [1, 16, 67]. Electrostatic force as a major force can cause the deposition of AgNPs being characterised with positive charge on the surface of adsorbent being characterised with negative charge [8, 41, 42, 52]. The AgNPs adsorption on *Aeromonas punctata* occurs because the aggregation of positively charged AgNPs interacts with negatively charged surface layers of *Aeromonas punctata* in the presence of anionic polyelectrolytes [41]. Adsorption process cannot occur when the reaction conditions of AgNPs and bacterial surface layers of *Aeromonas punctata* carry an identical positive charge. The forces of attraction or repulsion between AgNPs and bacterial extracellular proteins may occur depending on charge state distribution of the surface layers of *Aeromonas punctata* [52]. The mechanism of interaction between AgNPs and *Aeromonas punctata* controls the electrostatic attraction of AgNPs with their positive charge deposited on the bacterial surface layers with their negative charge [42].

Van der Waals interaction

The mechanism of AgNPs adsorption by commercial activated carbon (CAC) can be reasonably described using the van der Waals forces due to that the nature of CAC can fairly be classed as hydrophobic adsorbent. An investigation of the electrostatic interaction has been reported that the steric repulsive forces of ligand shell failed to prevent the deposition of AgNPs on the surface of CAC having relatively high ionic strengths [27]. Therefore, the mechanism of AgNPs deposited on CAC surface cannot be subjected to electrostatic forces. The hydrophobic property of CAC should be able to bind in a number of different adsorbates because the van der Waals interaction between CAC and adsorbate material exists. The nature of metal–carbon interactions investigated from the structure and surface properties of gold nanoparticles interacted with carbon nanotubes can be subjected to the van der Waals forces [99]. The mechanisms of AgNPs adsorption on absorbent are likely to depend on many factors including adsorbent dosage, contact time, ionic strength, pH, and water matrices.

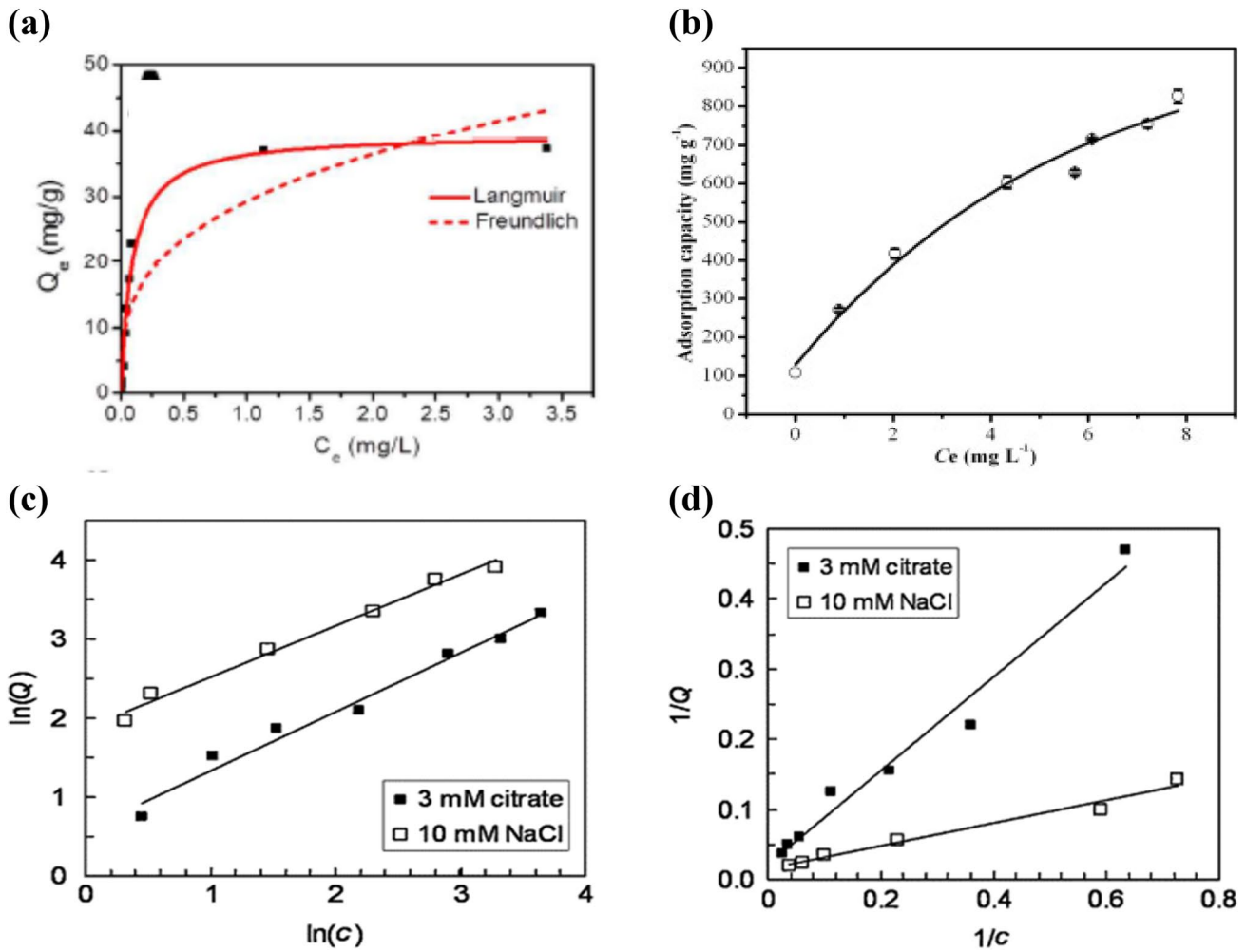

Fig. 4 Isotherm behaviours for the adsorption of AgNPs onto: **a** aged iron oxide magnetic particles described by the Langmuir and Freundlich models [100], **b** Fe_3O_4–SiO_2–PEI described by the Freundlich model [98], **c** Norit-CA1 described by the Freundlich model [27], and **d** Norit-CA1 described by the Langmuir model [27]

Table 3 Isotherm adsorption property of AgNPs deposited on various adsorbents

Adsorbent	C_e	q_m	References
Aeromonas punctata	0 to 30	0.05 to 0.44(1)	Khan et al. [41]
Activated carbon (Norit-CA1)	0 to 50	46 to 65	Gicheva and Yordanov [27]
Activated sludge	5 to 200	19.67 to 89.08	Oh et al. [66]
Aged iron oxide magnetic particles	0.01 to 15	19.90 to 62.90	Zhou et al. [100]
Glass beads	100 to 1000	6.93	Polowczyk et al. [72]
Sodium montmorillonite nanoclay	1 to 7	71.40	Zarei and Barghak [97]
Nitrogen-rich core–shell magnetic mesoporous silica	0 to 8	909.1	Zhang et al. [98]
Mussel-inspired Fe_3O_4–polydopamine core–shell microspheres	0 to 18	160.9	Wu et al. [94]
Poly(vinyl alcohol)	2 to 70	5.01	Dhandayuthapani et al. [14]
Poly(vinyl alcohol)/gluten nanofibers (2.5 wt%)	2 to 70	27.70	Dhandayuthapani et al. [14]
Poly(vinyl alcohol)/gluten nanofibers (5.0 wt%)	2 to 70	31.84	Dhandayuthapani et al. [14]

Remarks that the units of C_e are all expressed in mg L^{-1} and the units of q_m are all expressed in mg g^{-1} except(1) the unit of q_m for the adsorbent of *Aeromonas punctata* is expressed in the mean nuclear DNA content (pg) per cell (pg $cell^{-1}$)

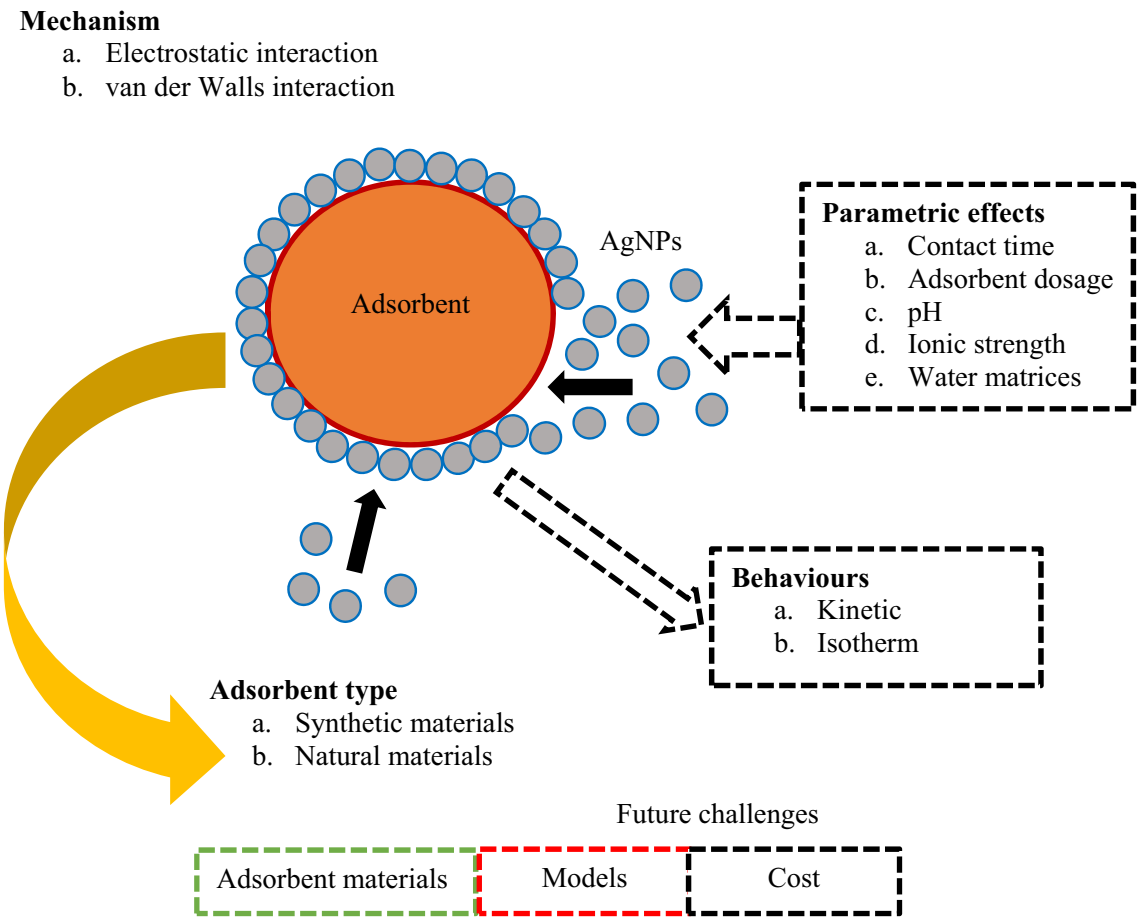

Fig. 5 An overview of AgNPs adsorption by the synthetic and natural adsorbent materials

Factors of adsorbent dosage, contact time, ionic strength, pH, and water matrices

Adsorbent dosage could be one of the important factors affecting the AgNPs deposited on both the synthetic and natural adsorbent materials. An increase in the adsorption efficiency from 25 to 75% is due to an increase in absorbent dosage from 1 to 175 g that can increase the number of active sites and surface area of the glass beads [72]. However, the adsorption capacity decreased with increase in the dosage of glass beads which is due to some adsorption sites remaining inactive during the adsorption process.

Effect of the various process parameters has been investigated by batch experiment for the deposition of AgNPs onto the surface of various materials. An increase in the contact time from 10 to 240 min can increase the efficiency of AgNPs adsorption on the surface of multiwalled carbon nanotubes from 57 to 88% [32]. The adsorption capacity of Fe_3O_4–polydopamine core–shell microspheres was verified to gradually increase along with the contact time increased up to 26 h and then to remain constant after 36 h of the contact time [94]. The deposition of AgNPs significantly increased at the beginning of adsorption process which could be because the abundant active sites on both the surface of multiwalled carbon nanotubes and Fe_3O_4–polydopamine core–shell microspheres are still available.

Surface charge influenced by the ionic strength of a solution is due to the adsorption process that can take place leading to have a difference in the electrical potential of inner to outer surface of dispersed phase in solution. Adsorption of AgNPs onto the synthetic or natural materials would be affected by ionic strength of altering the concentrations of such as $NaNO_3$, NaCl, $CaCl_2$, and $MgCl_2$ in solution. Adsorption capacity of AgNPs on the cell surface of *Aeromonas punctata* increased with increase in the NaCl concentration from 0 to 0.1 M in solution which could be because an attraction by electrostatic force favours the adsorption of AgNPs being characterised by positive charge on the bacterial cell surface being characterised by negative charge [41]. However, the adsorption capacity can gradually decrease when the NaCl concentration increases from 0.1 to 1.5 M that is because the degree of repulsion between AgNPs and bacterial cells surface continuously

increases [41]. Electrostatic barrier can limit the interaction of cell–particle due to the AgNPs and bacterial cell that are all positively charged when the concentration of NaCl in solution is high [41]. An increase in the concentration of NaCl generates the cations that cover the AgNPs species and bacterial surface to form a shield and can decrease the attractive forces [52].

Effect of pH on AgNPs removal by *Aeromonas punctata* shows that the capacity of AgNPs adsorption on the surface layers of *Aeromonas punctata* decreases with increase in pH, while a very low adsorption capacity was verified at pH 9. This is due to the surfaces of AgNPs, and bacterial extracellular proteins of *Aeromonas punctata* can exhibit a negative charge [41]. The balance between attractive and repulsive forces results in shielding without using a large number of AgNPs and thus decreases the adsorption capacity of AgNPs. The adsorption of AgNPs onto Fe_3O_4–polydopamine core–shell microspheres has been found to be depend on pH. An increase in the adsorption percentage of AgNPs can be attributed to the Ag–catechol bonds formation because of the existing of specifically high affinity between AgNPs and polydopamine on the Fe_3O_4 surface as the pH increases from 6 to 10 [94]. The percentage of AgNPs adsorption decreases when the pH is greater than 10 because the hindrance to the process of negatively charged AgNPs deposited on the surface of Fe_3O_4–polydopamine core–shell microspheres occurred under alkaline conditions of pH higher than 10.

Effect of the natural water matrices on the adsorption efficiency of AgNPs has been evaluated using the ultrapure water and river water from the Jialingjiang River to show that the adsorption capacity of AgNPs onto Fe_3O_4–PDA in the river water is almost similar to that in the ultrapure water [94].

Future challenges of AgNPs adsorption

Materials

In spite of many synthetic materials are commonly used as the adsorbents used to remove AgNPs from waters, the natural adsorbent-based materials with their abundant availability attained considerable attention for the water purification from AgNPs contamination. Application of the natural materials allows the market orientation and the development of porous structure because they have the advantages of well-defined surface chemistry, large surface area, homogeneous pore size distribution, and the easy preparation and regeneration to owning the multiple practices. The landscape of scientific research and funding in the future is in flux and affected by the availability of the natural adsorbent-based materials, involving the validity of both kinetic and isotherm models, and questions about regenerating adsorbent and adsorption capacity. Many natural materials of agricultural by-products and wood by-products can be modified by the sequential process comprising of carbonisation of the raw natural materials followed by activation of the carbonaceous char with the presence of chemicals or suitable oxidising gases at elevated temperatures to be more applicable to the removal of AgNPs from waters. The use of corncob silica of imbedded AgNPs can be used as the useful materials to inactivate bacteria [82]. In addition, the use of macrofungus can be encouraged for the removal of AgNPs because it provides a more meso- and macropore distribution and larger surface area compared to that of microfungus [90]. This review reveals that it has been no natural adsorbent materials of having the adsorption capacity better than synthetic adsorbent materials. However, still there is a need to find out the practical utility of the natural adsorbents with high adsorption capacity on an industrial scale, leading to the improvement of AgNPs adsorption in the best means of achieving the pollution prevention. Table 4 summarises the advantages and disadvantages of the natural and synthetic adsorbent materials to be used for the removal of AgNPs from waters.

Models

A review of the kinetic and isotherm models to validate the secondary data of different sources for the adsorption

Table 4 Summary of the advantages and disadvantages of the adsorbent materials

Type of adsorbent	Advantage	Disadvantage
Natural material	Abundantly available	Low adsorption capacity
	Easily accessible	Weaker for long-term use
	Easy preparation	
	Free of toxic	
	Low cost	
	Potential as new applicable material	
	Biodegradable	
Synthetic material	High adsorption capacity	Expensive
	Potential as new applicable material	Potential as new pollutant sources
	Stronger for long-term use	Complicated procedure

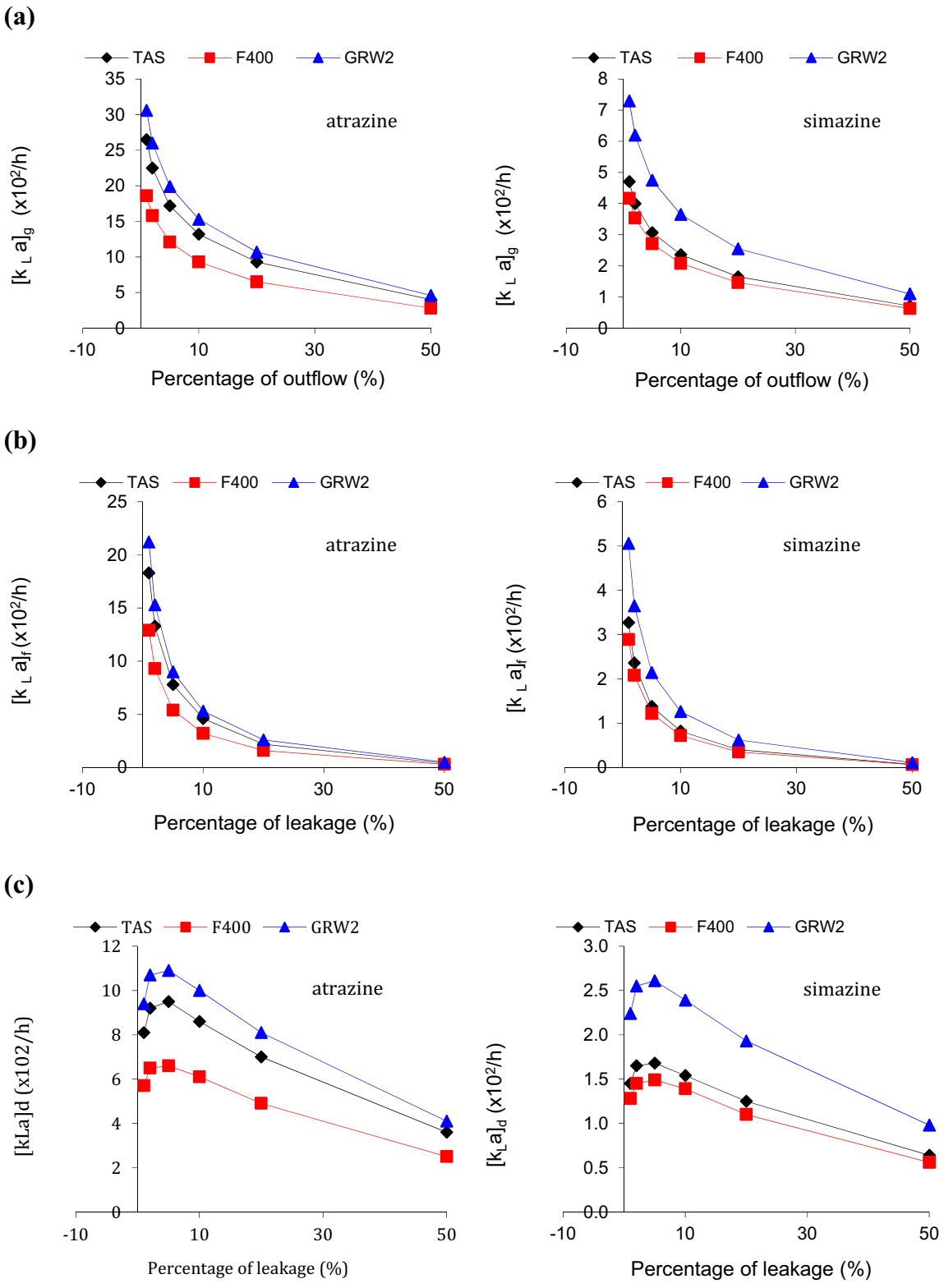

Fig. 6 Kinetic adsorption behaviours of atrazine and simazine deposited on granular activated carbon described by the MTF models with the variations of **a** $[k_L a]_g$, **b** $[k_L a]_f$, and **c** $[k_L a]_d$ pursuant to the percentage of outflow [19]

of AgNPs onto various adsorbents has shown an inconsistency of either the kinetic or isotherm models to describe the behaviours of AgNPs adsorption [89]. In spite of the use of the pseudo-second-order kinetic equation that has been discussed in this work can offer a better performance for the adsorption of AgNPs onto various synthetic materials, this kinetic model cannot match the experimental data of assessing the behaviour of AgNPs adsorption onto the natural material of *Aeromonas punctata*. Despite the use of the Langmuir isotherm model can be used to measure the capability of AgNPs adsorption processed by certain materials, this isotherm model cannot match the experimental data of assessing the characteristics of AgNPs adsorption onto the commercial activated carbon of Norit-CA1. This review reveals that the kinetic and isotherm models are still having a weakness because the mechanisms of adsorption of different adsorbates on the surface of an adsorbent are different. But it still remains a challenge for current environmentalists to find a more general equation to be used for describing the kinetic and isotherm behaviours of the AgNPs removal from water. Therefore, the use of the mass transfer factor (MTF) models that have been validated as the most reliable models to be used for studying the adsorptions of three kinds of surfactants [18] and two herbicides of atrazine and simazine [19] onto GAC in hydrodynamic column can be suggested for use in investigating the adsorption of AgNPs. Such models have been used also to study the isotherm adsorption of Cd(II) ions onto the beads of titania polyvinyl alcohol–alginate [23] in batch experiment. Figure 6 shows an example of the kinetic adsorption behaviours of atrazine and simazine deposited on granular activated carbon, which is best described using the MTF models [19]. This study suggested that the use of the MTF models is useful for describing the adsorption behaviours of AgNPs removal from non-contaminated water because it would be applicable to determine the resistance of mass transfer and to describe the mechanisms of external and internal mass transfer. Using the modified transfer factor (MMTF) models permits us to investigate the simultaneous adsorption of NH_4^+ and Al^{3+} [22] and the adsorption of phosphate [21] onto GAC from a contaminated water in hydrodynamic column. These models have been used also to study the biosorption of oil and grease from agro-food industrial processing effluent in plug flow reactor supported by *Serratia marcescens* SA30 strain [20] and the biosorption of nitrogenous and phosphorous matters from palm oil mill effluent in sequencing batch reactor supported by aerobic granules [24, 25]. Figure 7 shows as an example that the kinetic adsorption behaviours of NH_4^+ and Al^{3+} deposited on granular activated carbon can be perfectly described using the MMTF models [22]. This study convincingly suggested that both the MTF and MMTF models can be used to describe the kinetic behaviours of transporting AgNPs beginning from the bulk water and then ending after the fixation within the pores and can also determine the resistance of mass transfer. Table 5 summarises the most applicable kinetic and isotherm models that have

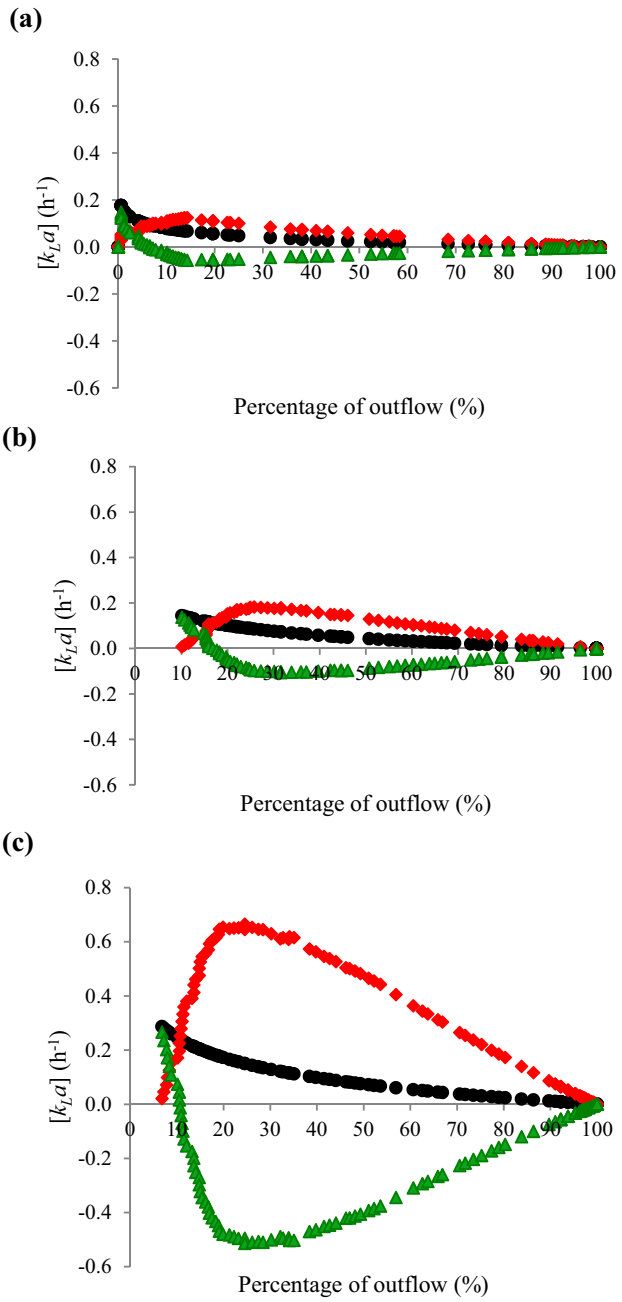

Fig. 7 Kinetic adsorption behaviours of NH_4^+ and Al^{3+} deposited on granular activated carbon described by the MMTF models with the variations of $[k_L a]_g$ (black), $[k_L a]_f$ (red), and $[k_L a]_d$ (green) pursuant to the percentage of outflow, where **a** the adsorption of NH_4^+ onto GAC from surface water, **b** the adsorption of Al^{3+} onto GAC from surface water, and **c** the simultaneous adsorption of NH_4^+ and Al^{3+} onto GAC from surface water [22] (color figure online)

Table 5 List of the most applicable kinetic and isotherm models to describe the adsorption of different adsorbates by different types of adsorbents

Model	Adsorbate	Adsorbent	Reference
Adsorption kinetics			
Power	Hexavalent chromium	Dead fungal biomass of marine *Aspergillus niger*	Khambhaty et al. [39]
Avrami	(1) Methylene blue and (2) Hg(II)	(1) Brazilian pine-fruit shell in natural and carbonised forms and (2) thin chitosan membranes	(1) Royer et al. [76] and (2) Lopes et al. [54]
Bangham	Anionic and cationic dyes	Activated carbon	Rodríguez et al. [75]
Mixed 1,2-order	Methylene blue	Mesoporous carbons	Marczewski [59]
Double-exponential	Cadmium ions	Duolite ES 467 resin	Haerifar and Azizian [29]
Fractal-like exponential	Cadmium ions	Duolite ES 467 resin	Haerifar and Azizian [29]
Boyd	Copper ions	Surface modified agricultural waste	Kumar et al. [45]
Fractal-like pseudo-first-order	ArNS–Cu	Heterogeneous solid surfaces	Haerifar and Azizian [30]
Fractal-like pseudo-second-order	ArNS–Cu	Heterogeneous solid surfaces	Haerifar and Azizian [30]
Fractal-like mixed 1,2-order	ArNS–Cu	Heterogeneous solid surfaces	Haerifar and Azizian [30]
Adsorption isotherm			
Langmuir–Freundlich	Arsenic	Pure goethite and goethite-coated sand	Jeppu and Clement [36]
Redlich–Peterson	Dyes	Fly ash and red mud	Wang et al. [92]
Toth	Basic red 9	Activated carbon derived from immature cotton seeds	Sivarajasekar and Baskar [86]
Khan	Phenol based organic pollutants	Activated carbon	Khan et al. [40]
Jovanovic	Benzoic acid	Granular activated carbon	Shahbeig et al. [79]
Koble–Corrigan	Pure hydrocarbons	Activated charcoal	Koble and Corrigan [43]
Radke–Prausnitz	Organic solutes	Activated carbon	Radke and Prausnitz [74]
Fritz–Schlunder	Organic solutes	Activated carbon	Fritz and Schluender [17]
Baudu	Basic red 9	Activated carbon derived from immature cotton seeds	Sivarajasekar and Baskar [86]
Marczewski–Jaroniec	Basic red 9	Activated carbon derived from immature cotton seeds	Sivarajasekar and Baskar [86]
Hill	Haemoglobin	Salts present in the solution	Hill [34]
Brouers–Sotolongo	As(III) and As(V)	Novel neem leaves/$MnFe_2O_4$ composite biosorbent	Podder and Majumder [70]
Unilin	Basic red 9	Activated carbon derived from immature cotton seeds	Sivarajasekar and Baskar [86]

been used to describe the adsorption of different adsorbates by different types of adsorbents. Furthermore, it has been reviewed the applicability of the fifteen kinetic models and fifteen isotherm models to explain the behaviours of AgNPs deposited on the various adsorbent materials [89] to show that the applicability of a model is dependent on the nature and characteristics of the adsorbent.

Cost

The price of the natural cover the costs necessary to manufacture the adsorbents adsorbent-based materials not only has to but also the other costs of such as administrative overhead and cost of adsorption process. A large number of various natural materials-based adsorbents have been suggested for determining their ability to remove the contamination of AgNPs from waters. Several types of the natural materials and typical waste products from certain industries can be modified to activated carbons for use as the adsorbent materials in removing AgNPs from contaminated water because such types of the raw adsorbent materials can be easily obtained, prepared, employed, and disposed them with a little cost [4]. A comprehensive guideline for carrying out cost–benefit analysis can be suggested for the whole process of AgNPs adsorption on the various natural adsorbent materials in order to get better understanding on the capital and operating costs affected by different parameters. The analysis of catalyst production in the biocatalytic processes by the guidelines and cost analysis has exhibited that the reduction in production costs for the adsorption of AgNPs by several orders

of magnitude would be possible and has the potential to achieve the markets potential of the products [91]. This review reveals that there are no economic studies to analyse whether the adsorption of AgNPs onto various natural adsorbents would be applicable to an industrial scale. It therefore provides a suggestion for the future of AgNPs adsorption regarding the methodological solutions on how to analyse the economics of AgNPs deposited on the surface of low-cost adsorbents prepared from various natural materials.

Conclusions

This paper reviewed the adsorption of AgNPs onto the various synthetic and natural materials to reveal the interaction of AgNPs with halides, oxygen, and sulphide depending on the environmental conditions. The validity of the adsorption kinetics and isotherm models depends on the nature of the adsorbent materials. The performance of AgNPs adsorption is controlled by the interaction mechanisms of either electrostatic or van der Waals forces and affected by the factors of contact time, adsorbent dosage, pH, ionic strength, and natural water matrices. This review provides a valuable insight into the future challenges of AgNPs adsorption regarding the adsorbent materials, the kinetics and isotherm models, and the costs analysis. The MTF and MMTF models can specifically be suggested for use in the analysis of the behaviours of AgNPs adsorption by natural material-based adsorbents to get better understanding of the environmental remediation in the future. The future applications of the natural adsorbent materials, kinetics and isotherm models, and manufacturing cost analysis have been suggested towards contributing to the improvement of AgNPs deposited on various natural materials.

Acknowledgements The authors thank the Malaysian Ministry of Higher Education for supporting this study by the Fundamental Research Grant Scheme (FRGS) Vot. No. 4F619, the Universiti Teknologi Malaysia by the Research University Grant (GUP) Vot. No. 18H92, and the Ton Duc Thang University by the Contract No. 551/2019/TĐT-HĐLV-NCV.

Compliance with ethical standards

Conflict of interest All authors declare that they have no conflict of interest.

References

1. Adamczyk Z (2003) Particle adsorption and deposition: role of electrostatic interactions. Adv Colloid Interface Sci 100–102:267–347
2. Ahmed S, Ahmad M, Swami BL, Ikram S (2016) A review on plants extract mediated synthesis of silver nanoparticles for antimicrobial applications: a green expertise. J Adv Res 7:17–28
3. Appapalam ST, Panchamoorthy R (2017) Aerva lanata mediated phytofabrication of silver nanoparticles and evaluation of their antibacterial activity against wound associated bacteria. J Taiwan Inst Chem Eng 78:539–551
4. Bailey SE, Olin TJ, Bricka RM, Adrian DD (1999) A review of potentially low-cost sorbents for heavy metals. Water Res 33:2469–2479
5. Blaser SA, Scheringer M, MacLeod M, Hungerbühler K (2008) Estimation of cumulative aquatic exposure and risk due to silver: contribution of nano-functionalized plastics and textiles. Sci Total Environ 390:396–409
6. Bouabidi ZB, El-Naas MH, Cortes D, McKay G (2018) Steelmaking dust as a potential adsorbent for the removal of lead(II) from an aqueous solution. Chem Eng J 334:837–844
7. Bozyigit D, Yazdani N, Yarema M, Yarema O, Lin WMM, Volk S et al (2016) Soft surfaces of nanomaterials enable strong phonon interactions. Nature 531:618–622
8. Brenner T, Paulus M, Schroer MA, Tiemeyer S, Sternemann C, Möller J et al (2012) Adsorption of nanoparticles at the solid–liquid interface. J Colloid Interface Sci 374:287–290
9. Chang C-W, Cheng T-Y, Liao Y-C (2018) Encapsulated silver nanoparticles in water/oil emulsion for conductive inks. J Taiwan Inst Chem Eng 92:8–14
10. Chen SF, Zhang H, Lin QY (2013) Effect of different water conditions on dissolution of nanosilver. Water Sci Technol 68:1745–1750
11. Choi O, Clevenger TE, Deng B, Surampalli RY, Ross L, Hu Z (2009) Role of sulfide and ligand strength in controlling nanosilver toxicity. Water Res 43:1879–1886
12. Conde-González J, Peña-Méndez E, Rybáková S, Pasán J, Ruiz-Pérez C, Havel J (2016) Adsorption of silver nanoparticles from aqueous solution on copper-based metal organic frameworks (HKUST-1). Chemosphere 150:659–666
13. Desireddy A, Conn BE, Guo J, Yoon B, Barnett RN, Monahan BM et al (2013) Ultrastable silver nanoparticles. Nature 501:399–402
14. Dhandayuthapani B, Mallampati R, Sriramulu D, Dsouza RF, Valiyaveettil S (2014) PVA/gluten hybrid nanofibers for removal of nanoparticles from water. ACS Sustain Chem Eng 2:1014–1021
15. Dobias J, Bernier-Latmani R (2013) Silver release from silver nanoparticles in natural waters. Environ Sci Technol 47:4140–4146
16. Dugyala VR, Muthukuru JS, Mani E, Basavaraj MG (2016) Role of electrostatic interactions in the adsorption kinetics of nanoparticles at fluid–fluid interfaces. Phys Chem Chem Phys 18:5499–5508
17. Fritz W, Schluender EU (1974) Simultaneous adsorption equilibria of organic solutes in dilute aqueous solutions on activated carbon. Chem Eng Sci 29:1279–1282
18. Fulazzaky MA (2011) Determining the resistance of mass transfer for adsorption of the surfactant onto granular activated carbons from hydrodynamic column. Chem Eng J 166:832–840
19. Fulazzaky MA (2012) Analysis of global and sequential mass transfers for the adsorption of atrazine and simazine onto granular activated carbons from hydrodynamic column. Anal Methods 4:2396–2403
20. Fulazzaky MA, Abdullah S, Salim MR (2015) Fundamentals of mass transfer and kinetics for biosorption of oil and grease from agro-food industrial effluent by *Serratia marcescens* SA30. RSC Adv 5:104666–104673
21. Fulazzaky MA, Khamidun MH, Din MFM, Yusoff ARM (2014) Adsorption of phosphate from domestic wastewater treatment

plant effluent onto the laterites in a hydrodynamic column. Chem Eng J 258:10–17
22. Fulazzaky MA, Khamidun MH, Omar R (2013) Understanding of mass transfer resistance for the adsorption of solute onto porous material from the modified mass transfer factor models. Chem Eng J 228:1023–1029
23. Fulazzaky MA, Majidnia Z, Idris A (2017) Mass transfer kinetics of Cd(II) ions adsorption by titania polyvinylalcohol–alginate beads from aqueous solution. Chem Eng J 308:700–709
24. Fulazzaky MA, Nuid M, Aris A, Muda K (2018) Mass transfer kinetics of biosorption of nitrogenous matter from palm oil mill effluent by aerobic granules in sequencing batch reactor. Environ Technol 39:2151–2161
25. Fulazzaky MA, Nuid M, Aris A, Fulazzaky M, Sumeru K, Muda K (2019) Mass transfer kinetics of phosphorus biosorption by aerobic granules. J Water Process Eng 31:100889
26. Garg S, Rong H, Miller CJ, Waite TD (2016) Oxidative dissolution of silver nanoparticles by chlorine: implications to silver nanoparticle fate and toxicity. Environ Sci Technol 50:3890–3896
27. Gicheva G, Yordanov G (2013) Removal of citrate-coated silver nanoparticles from aqueous dispersions by using activated carbon. Colloids Surf A Physicochem Eng Aspects 431:51–59
28. Gomaa OM (2014) Removal of silver nanoparticles using live and heat shock *Aspergillus niger* cultures. World J Microbiol Biotechnol 30:1747–1754
29. Haerifar M, Azizian S (2013) An exponential kinetic model for adsorption at solid/solution interface. Chem Eng J 215–216:65–71
30. Haerifar M, Azizian S (2014) Fractal-like kinetics for adsorption on heterogeneous solid surfaces. J Phys Chem C 118:1129–1134
31. Hameed BH, Tan IAW, Ahmad AL (2008) Adsorption isotherm, kinetic modeling and mechanism of 2,4,6-trichlorophenol on coconut husk-based activated carbon. Chem Eng J 144:235–244
32. Hassan DM, Farghali MR (2017) Adsorption of silver nanoparticles from aqueous solution by multiwalled carbon nanotubes. Adv Nanopart 6:22–32
33. Hefne J, Mekhemer W, Alandis N, Aldayel O, Alajyan T (2010) Removal of silver(I) from aqueous solutions by natural bentonite. Science 22:155–176
34. Hill AV (1910) The possible effects of the aggregation of the molecules of haemoglobin on its oxygen dissociation curve. J Physiol 40:4–7
35. Ho C-M, Yau SK-W, Lok C-N, So M-H, Che C-M (2010) Oxidative dissolution of silver nanoparticles by biologically relevant oxidants: a kinetic and mechanistic study. Chem Asian J 5:285–293
36. Jeppu GP, Clement TP (2012) A modified Langmuir–Freundlich isotherm model for simulating pH-dependent adsorption effects. J Contam Hydrol 129:46–53
37. Kaegi R, Voegelin A, Ort C, Sinnet B, Thalmann B, Krismer J et al (2013) Fate and transformation of silver nanoparticles in urban wastewater systems. Water Res 47:3866–3877
38. Keat CL, Aziz A, Eid AM, Elmarzugi NA (2015) Biosynthesis of nanoparticles and silver nanoparticles. Bioresour Bioprocess 2:47
39. Khambhaty Y, Mody K, Basha S, Jha B (2009) Kinetics, equilibrium and thermodynamic studies on biosorption of hexavalent chromium by dead fungal biomass of marine *Aspergillus niger*. Chem Eng J 145:489–495
40. Khan AR, Al-Bahri TA, Al-Haddad A (1997) Adsorption of phenol based organic pollutants on activated carbon from multi-component dilute aqueous solutions. Water Res 31:2102–2112
41. Khan SS, Mukherjee A, Chandrasekaran N (2012) Adsorptive removal of silver nanoparticles (SNPs) from aqueous solution by *Aeromonas punctata* and its adsorption isotherm and kinetics. Colloids Surf B 92:156–160
42. Khan SS, Srivatsan P, Vaishnavi N, Mukherjee A, Chandrasekaran N (2011) Interaction of silver nanoparticles (SNPs) with bacterial extracellular proteins (ECPs) and its adsorption isotherms and kinetics. J Hazard Mater 192:299–306
43. Koble RA, Corrigan TE (1952) Adsorption isotherms for pure hydrocarbons. Ind Eng Chem 44:383–387
44. Kumar A, Vemula PK, Ajayan PM, John G (2008) Silver-nanoparticle-embedded antimicrobial paints based on vegetable oil. Nat Mater 7:236–241
45. Kumar PS, Senthamarai C, Durgadevi A (2014) Adsorption kinetics, mechanism, isotherm, and thermodynamic analysis of copper ions onto the surface modified agricultural waste. Environ Prog Sustain Energy 33:28–37
46. Lei Y, Mehmood F, Lee S, Greeley J, Lee B, Seifert S et al (2010) Increased silver activity for direct propylene epoxidation via subnanometer size effects. Science 328:224–228
47. Levard C, Hotze EM, Lowry GV, Brown GE (2012) Environmental transformations of silver nanoparticles: impact on stability and toxicity. Environ Sci Technol 46:6900–6914
48. Levard C, Mitra S, Yang T, Jew AD, Badireddy AR, Lowry GV et al (2013) Effect of chloride on the dissolution rate of silver nanoparticles and toxicity to *E. coli*. Environ Sci Technol 47:5738–5745
49. Li L, Zhou Q, Geng F, Wang Y, Jiang G (2016) Formation of nanosilver from silver sulfide nanoparticles in natural waters by photoinduced Fe(II, III) redox cycling. Environ Sci Technol 50:13342–13350
50. Li X, Yang Z, Peng Y (2018) The interaction of silver nanoparticles with papain and bromelain. New J Chem 42:4940–4950
51. Liu H-H, Li Q, Liang X, Xiong X, Yu J, Guo Z-X (2016) Antibacterial polycaprolactone electrospun fiber mats prepared by soluble eggshell membrane protein-assisted adsorption of silver nanoparticles. J Appl Polym Sci 133:43850
52. Liu H-S, Wang Y-C, Chen W-Y (1995) The sorption of lysozyme and ribonuclease onto ferromagnetic nickel powder 1. Adsorption of single components. Colloids Surf B 5:25–34
53. Liu J, Hurt RH (2010) Ion release kinetics and particle persistence in aqueous nano-silver colloids. Environ Sci Technol 44:2169–2175
54. Lopes ECN, dos Anjos FSC, Vieira EFS, Cestari AR (2003) An alternative Avrami equation to evaluate kinetic parameters of the interaction of Hg(II) with thin chitosan membranes. J Colloid Interface Sci 263:542–547
55. Lopes JL, Marques KL, Girão AV, Pereira E, Trindade T (2016) Functionalized magnetite particles for adsorption of colloidal noble metal nanoparticles. J Colloid Interface Sci 475:96–103
56. Ma R, Levard C, Judy JD, Unrine JM, Durenkamp M, Martin B et al (2014) Fate of zinc oxide and silver nanoparticles in a pilot wastewater treatment plant and in processed biosolids. Environ Sci Technol 48:104–112
57. Mahanta N, Valiyaveettil S (2011) Surface modified electrospun poly(vinylalcohol) membranes for extracting nanoparticles from water. Nanoscale 3:4625–4631
58. Mallampati R, Valiyaveettil S (2013) Biomimetic metal oxides for the extraction of nanoparticles from water. Nanoscale 5:3395–3399
59. Marczewski AW (2010) Application of mixed order rate equations to adsorption of methylene blue on mesoporous carbons. Appl Surf Sci 256:5145–5152
60. Matias MS, Melegari SP, Vicentini DS, Matias WG, Ricordel C, Hauchard D (2015) Synthetic wastewaters treatment by electrocoagulation to remove silver nanoparticles produced by different routes. J Environ Manage 159:147–157

61. Metcalfe CD, Sultana T, Martin J, Newman K, Helm P, Kleywegt S et al (2018) Silver near municipal wastewater discharges into western Lake Ontario, Canada. Environ Monit Assess 190:555
62. Moustafa MT (2017) Removal of pathogenic bacteria from wastewater using silver nanoparticles synthesized by two fungal species. Water Sci 31:164–176
63. Naik RR, Stringer SJ, Agarwal G, Jones SE, Stone MO (2002) Biomimetic synthesis and patterning of silver nanoparticles. Nat Mater 1:169–172
64. Ng C, Losso JN, Marshall WE, Rao RM (2002) Freundlich adsorption isotherms of agricultural by-product-based powdered activated carbons in a geosmin–water system. Biores Technol 85:131–135
65. Nguyen N-T, Liu J-H (2014) A green method for in situ synthesis of poly(vinylalcohol)/chitosan hydrogel thin films with entrapped silver nanoparticles. J Taiwan Inst Chem Eng 45:2827–2833
66. Oh SY, Sung HK, Park C, Kim Y (2015) Biosorptive removal of bare-, citrate-, and PVP-coated silver nanoparticles from aqueous solution by activated sludge. J Ind Eng Chem 25:51–55
67. Osaki T, Renner L, Herklotz M, Werner C (2006) Hydrophobic and electrostatic interactions in the adsorption of fibronectin at maleic acid copolymer films. J Phys Chem B 110:12119–12124
68. Padil VVT, Černík M (2015) Poly(vinyl alcohol)/gum karaya electrospun plasma treated membrane for the removal of nanoparticles (Au, Ag, Pt, CuO and Fe_3O_4) from aqueous solutions. J Hazard Mater 287:102–110
69. Padil VVT, Stuchlík M, Černík M (2015) Plasma modified nanofibres based on gum kondagogu and their use for collection of nanoparticulate silver, gold and platinum. Carbohydr Polym 121:468–476
70. Podder MS, Majumder CB (2016) Sequestering of As(III) and As(V) from wastewater using a novel neem leaves/$MnFe_2O_4$ composite biosorbent. Int J Phytorem 18:1237–1257
71. Polo AMS, Lopez-Peñalver JJ, Rivera-Utrilla J, Von Gunten U, Sánchez-Polo M (2017) Halide removal from waters by silver nanoparticles and hydrogen peroxide. Sci Total Environ 607–608:649–657
72. Polowczyk I, Koźlecki T, Bastrzyk A (2015) Adsorption of silver nanoparticles on glass beads surface. Adsorpt Sci Technol 33:731–737
73. Qureshi ZS, Dsouza R, Mallampati R, Valiyaveettil S (2014) Synthesis of amine-functionalized block copolymers for nanopollutant removal from water. J Appl Polym Sci 131:40943
74. Radke CJ, Prausnitz JM (1972) Adsorption of organic solutes from dilute aqueous solution on activated carbon. Ind Eng Chem Fundam 11:445–451
75. Rodríguez A, García J, Ovejero G, Mestanza M (2009) Adsorption of anionic and cationic dyes on activated carbon from aqueous solutions: equilibrium and kinetics. J Hazard Mater 172:1311–1320
76. Royer B, Cardoso NF, Lima EC, Vaghetti JCP, Simon NM, Calvete T et al (2009) Applications of Brazilian pine-fruit shell in natural and carbonized forms as adsorbents to removal of methylene blue from aqueous solutions—kinetic and equilibrium study. J Hazard Mater 164:1213–1222
77. Ruíz-Baltazar A, Reyes-López SY, Tellez-Vasquez O, Esparza R, Rosas G, Pérez R (2015) Analysis for the sorption kinetics of Ag nanoparticles on natural clinoptilolite. Adv Condens Matter Phys 2015:284518
78. Setyono D, Valiyaveettil S (2016) Functionalized paper—a readily accessible adsorbent for removal of dissolved heavy metal salts and nanoparticles from water. J Hazard Mater 302:120–128
79. Shahbeig H, Bagheri N, Ghorbanian SA, Hallajisani A, Poorkarimi S (2013) A new adsorption isotherm model of aqueous solutions on granular activated carbon. World J Model Simul 9:243–254
80. Sharma VK, Filip J, Zboril R, Varma RS (2015) Natural inorganic nanoparticles-formation, fate, and toxicity in the environment. Chem Soc Rev 44:8410–8423
81. Sheng Z, Liu Y (2017) Potential impacts of silver nanoparticles on bacteria in the aquatic environment. J Environ Manag 191:290–296
82. Shim J, Mazumder P, Kumar M (2018) Corn cob silica as an antibacterial support for silver nanoparticles: efficacy on *Escherichia coli* and *Listeria monocytogenes*. Environ Monit Assess 190:583
83. Silva SM, Sampaio KA, Ceriani R, Verbé R, Stevens C, De Greyt W et al (2013) Adsorption of carotenes and phosphorus from palm oil onto acid activated bleaching earth: equilibrium, kinetics and thermodynamics. J Food Eng 118:341–349
84. Sim JH, Umh HN, Shin HH, Sung HK, Oh SY, Lee B-C et al (2014) Comparison of adsorptive features between silver ion and silver nanoparticles on nanoporous materials. J Ind Eng Chem 20:2864–2869
85. Simonin J-P (2016) On the comparison of pseudo-first order and pseudo-second order rate laws in the modeling of adsorption kinetics. Chem Eng J 300:254–263
86. Sivarajasekar N, Baskar R (2014) Adsorption of basic red 9 onto activated carbon derived from immature cotton seeds: isotherm studies and error analysis. Desalin Water Treat 52:7743–7765
87. Sun Q, Li Y, Tang T, Yuan Z, Yu C-P (2013) Removal of silver nanoparticles by coagulation processes. J Hazard Mater 261:414–420
88. Syafiuddin A, Salmiati S, Hadibarata T, Kueh ABH, Salim MR (2018) Novel weed-extracted silver nanoparticles and their antibacterial appraisal against a rare bacterium from river and sewage treatment plan. Nanomaterials 8:E9
89. Syafiuddin A, Salmiati S, Jonbi J, Fulazzaky MA (2018) Application of the kinetic and isotherm models for better understanding of the behaviors of silver nanoparticles adsorption onto different adsorbents. J Environ Manag 218:59–70
90. Sytu MRC, Camacho DH (2018) Green synthesis of silver nanoparticles (AgNPs) from *Lenzites betulina* and the potential synergistic effect of AgNP and capping biomolecules in enhancing antioxidant activity. BioNanoScience 8:835–844
91. Tufvesson P, Lima-Ramos J, Nordblad M, Woodley JM (2011) Guidelines and cost analysis for catalyst production in biocatalytic processes. Organ Process Res Dev 15:266–274
92. Wang S, Boyjoo Y, Choueib A, Zhu ZH (2005) Removal of dyes from aqueous solution using fly ash and red mud. Water Res 39:129–138
93. Wang T-H, Li M-H, Teng S-P (2009) Bridging the gap between batch and column experiments: a case study of Cs adsorption on granite. J Hazard Mater 161:409–415
94. Wu M, Li Y, Yue R, Zhang X, Huang Y (2017) Removal of silver nanoparticles by mussel-inspired Fe_3O_4@polydopamine core–shell microspheres and its use as efficient catalyst for methylene blue reduction. Sci Rep 7:42773
95. Xiang L, Fang J, Cheng H (2018) Toxicity of silver nanoparticles to green algae *M. aeruginosa* and alleviation by organic matter. Environ Monit Assess 190:667
96. Xiao B, Dai Q, Yu X, Yu P, Zhai S, Liu R et al (2018) Effects of sludge thermal-alkaline pretreatment on cationic red X-GRL adsorption onto pyrolysis biochar of sewage sludge. J Hazard Mater 343:347–355
97. Zarei AR, Barghak F (2015) Fast and efficient adsorption of Ag nanoparticles by sodium montmorillonite nanoclay from aqueous systems. J Chem Res 39:542–545
98. Zhang X, Zhang Y, Zhang X, Li S, Huang Y (2017) Nitrogen rich core–shell magnetic mesoporous silica as an effective adsorbent for removal of silver nanoparticles from water. J Hazard Mater 337:1–9

99. Zhang Y, Franklin NW, Chen RJ, Dai H (2000) Metal coating on suspended carbon nanotubes and its implication to metal-tube interaction. Chem Phys Lett 331:35–41
100. Zhou XX, Li YJ, Liu JF (2017) Highly efficient removal of silver-containing nanoparticles in waters by aged iron oxide magnetic particles. ACS Sustain Chem Eng 5:5468–5476